

## Estimation of Radiative Forcing due to Aerosols over Selected Sites in Kenya

J. W. Makokha, J. N. Kimani and H. K. Angeyo

*Department of Physics, University of Nairobi*

### **CORRESPONDING AUTHOR**

**J. W. Makokha**

*Department of Physics, University of Nairobi*

*P.O. Box 30197-00100, Nairobi, Kenya*

(Manuscript received 19 October 2010, in final form 17 January 2011)

### **ABSTRACT**

Atmospheric aerosols modulate the radiative budget and ambient air quality of the atmosphere, thus, there is a need to develop both analytical and computational methodological techniques that determine their physical, chemical, optical and radiative properties in order to characterize and model their environmental effects. This paper embodies the results of the derivation of radiative characteristics of the atmosphere over Nairobi, Mbita and Malindi using aerosol data obtained from sun spectrophotometry from 2006-2008. Aerosol optical depths ( $\tau$ ), single scattering albedo ( $\omega$ ), angstrom exponent ( $\alpha$ ), asymmetry factor ( $g$ ) at zero Solar Zenith Angle (SZA) were derived through AErosol RObotic NETwork (AERONET) framework. The Coupled Ocean and Atmosphere Radiative Transfer (COART) model was then used to solve a radiative transfer equation (RTE) for an atmosphere modulated by aerosols of different particle sizes. Utilizing the integrated fluxes, radiative forcing due to atmospheric aerosols was estimated, and found to remain relatively constant at  $0.46 \text{ K}/(\text{W}/\text{m}^2)$  for all the three sites despite the observed differences in the various aerosol particle properties that is physical, mode of generation, chemical and number densities dominating the sites. This value was slightly lower as compared to the combined global anthropogenic radiative forcing estimated to be  $+1.6 [-1.0, +0.8] \text{ W}/\text{m}^2$ .

**Keywords:** Radiative forcing; integrated fluxes; radiative characteristics, Kenyan atmosphere

---

### **1. Introduction**

Aerosols directly affect the radiation budget of the atmosphere by absorbing and scattering solar radiation. Scattering of incoming solar radiation by aerosols yields a cooling effect on the Earth's atmosphere, while its absorption yields a warming effect. These effects are highly dependent on the coupled influences of the physical, chemical and optical properties of the predominant atmospheric aerosol types over a given region. Aerosols also indirectly modulate the radiative budget of the Earth by modifying the properties of clouds. They do this by acting as Cloud Condensation Nuclei (CCN), which aid in the formation of cloud droplets (Alpert *et al.*, 1998). A constant liquid content acts as an enhancement in the cloud dr-

oplet number through CCN which leads to an increase in cloud albedo. This indirect effect is also known as Twomey effect (Twomey, 1991).

Radiative forcing is the change in net (down minus up) irradiance (solar plus long-wave; in  $\text{W}/\text{m}^2$ ) at the top of the Earth's atmosphere or surface, due to secular changes in the atmospheric concentration of radiative active species e.g. aerosols. Global mean radiative forcing due to indirect aerosol effects ranges from 0 to  $-2 \text{ W}/\text{m}^2$  inclusive of ice and mixed phase clouds, though the magnitude of any indirect effect associated with ice phase is not known (IPCC, 2001). The total spectral irradiance (TSI) at the Earth's orbit can be calculated knowing the sun's radius, the photospheric temperature

and the value of earth-sun distance; the result is approximately  $1367 \text{ W/m}^2$ , with satellite observations indicating an average value of  $1367 \pm 4 \text{ W/m}^2$ . The impact of aerosols on climate depends on the radiative characteristics of the dominant aerosols over the atmosphere. The global annual mean direct radiative forcing for five distinct aerosols is outlined by IPCC (2001). It shows that the direction of the annual mean direct radiative forcing is aerosol particle composition dependent.

Studies reported by Hatzianastassiou *et al.* (2004) show that the atmosphere is heated by aerosols as much as  $25 \text{ W/m}^2$  with the highest values noted over areas characterized by strong absorbing mineral particles and high surface albedo (e.g., Sahara). It was also noted that the downward solar radiation at the Earth's surface was drastically reduced due to the presence of aerosols by up to  $30 \text{ W/m}^2$  (with the largest decrease noted over regions with high aerosol optical depths ( $\tau$ )). An increase in relative humidity increases the outgoing solar radiation over oceans through increased aerosol scattering from about  $1 \text{ W/m}^2$  to  $2 \text{ W/m}^2$ . The combined anthropogenic radiative forcing was estimated to be  $+1.6$  ( $-1.0$ ,  $+0.8$ )  $\text{W/m}^2$ . This indicated that between 1750 and 2005, humans have exerted a substantial warming influence on climate (Forster *et al.*, 2007).

For sulfate dominated aerosols, most of the recent estimates yield a cooling effect of below  $0.5 \text{ W/m}^2$  on a global scale, which is due to the scattering of the incoming solar radiation (Haywood *et al.*, 1997). It is also estimated that a mixture of sulfates and soot dominated aerosols (Hansen *et al.*, 1997; Haywood *et al.*, 1997) results in a warming of about  $0.2 \text{ W/m}^2$ . The radiative forcing due to sulfate aerosols is  $-0.32 \text{ W/m}^2$  while that of fossil fuel soot dominated aerosols is  $0.16 \text{ W/m}^2$ , according to the recent three dimensional chemistry transport model calculation (Myhre *et al.*, 1998). Calculated radiative forcing due to exte-

rnal and internal mixture of sulfate and soot aerosols amounts to about  $-0.18 \text{ W/m}^2$  and  $-0.02 \text{ W/m}^2$  respectively (Haywood *et al.*, 1997). On the other hand, radiative forcing due to mixture of sulfate and soot as an external mixture was estimated as  $-0.16 \text{ W/m}^2$  while an internal mixture for the same amounted to  $0.10 \text{ W/m}^2$  (Myhre *et al.*, 1998). Radiative transfer modeling through the Dust and Biomass-burning Experiment (DABEX) by Johnson *et al.* (2009) over West Africa suggested a  $130\text{-}160 \text{ W/m}^2$  instantaneous reduction of downwelling solar radiation by aerosol columns (15-18% of the total flux).

The aerosol optical properties that is aerosol optical depths ( $\tau$ ), single scattering albedo ( $\omega$ ), angstrom exponent ( $\alpha$ ), asymmetry factor ( $g$ ) at zero Solar Zenith Angle (SZA) that were used to derive the integrated flux were obtained in the AERONET framework (Holben *et al.*, 1998). The AERONET measurement system is a solar-powered weather hardy robotically pointed sun and sky radiometer based on the CIMEL Electronique 318A technique. This instrument has approximately a  $1.2^\circ$  full field of view and two silicon detectors for measurement of direct sun, aureole and sky radiance. It utilizes 33 cm collimators which are designed for  $10^{-5}$  stray light rejection for measurements of aureole  $3^\circ$  from the sun. A robot mounted sensor head is parked pointed nadir when idle to prevent contamination of optical windows from rain and foreign particles. The radiometer makes only two basic measurements, either directly sun or sky, both within several programmed sequences that are discussed in detail (Holben *et al.*, 1998). The main objectives of AERONET are to assess aerosol optical properties, and validate satellite retrievals of aerosol optical parameters based on its ground measurements (Holben *et al.*, 2001).

The knowledge of radiative forcing of the atmosphere is key in the development of climate models that are used for prediction of climate change and modeling of aerosol impact

on environmental pollution and human health. To obtain the integrated fluxes, a solution of a basic Radiative Transfer Equation (RTE) according to the COART model was utilized. This was obtained under different assumptions i.e. a homogeneous atmosphere, whose radiative characteristics is purely modulated by atmospheric aerosols; flat Earth surface and single layered atmosphere and plane parallel geometry as discussed by Zhonghai *et al.* (1994; 2006). Integrated fluxes together with equilibrium global mean surface temperature change ( $\Delta T_s = -3^\circ$ ) as estimated in the Fourth Assessment Report of the Intergovernmental Panel on Climate Change (IPCC) were used.

To understand the radiative properties of an atmosphere under study, there are a number of aerosol campaigns, besides AERONET, that furnish information on aerosol optical properties through passive remote sensing. These include ground-based spectroscopic techniques such as the Multi-axis Differential Optical Absorption Spectroscopy (MAX-DOAS) which may be used to retrieve aerosol profiles. The MAX-DOAS network has stations at different latitudes which can also be used for validation of satellite-based measurements of trace gases (Witrock *et al.*, 2004). Indirect and Semi-Direct Aerosol Campaigns (ISDAC) is an intensive cloud and aerosol observing system that facilitates both aerosol and cloud studies over the North Slope Alaska. Carbonaceous Aerosol and Radiative Effects Study (CARES) on the other hand is centered on making field measurements of different types of atmospheric carbonaceous aerosols and their climate effects (Ghan *et al.*, 2008).

A number of operational satellite sensors are also available from NASA. These include Total Ozone Mapping Spectrometer (TOMS) (Bowman and Krueger, 1985), Moderate Resolution Imaging Spectrometer (MODIS) on Aqua and Terra satellites (Badarinath *et al.*, 2009) and Multi-angle Imaging Spectrometer (MISR) (Wickland (1991)) that is a-board instrument of

the Earth Observing System (EOS) spacecraft providing a globally, radiometrically calibrated, geo-rectified and co-registered imagery at nine viewing angles and four Vis-NIR spectral bands. Satellite-borne measurements have the advantage that they can cover the entire earth in a day although only one or two observations can be made on a given position each day. Both ground and satellite based observations are vital for different situations as well as for cross-validation of each other. AERONET, which is a ground based network, was used in this study not only because of its availability over the sites under consideration but also due to the fact that we can obtain data as many times as possible over the sites of study per day. This aids in the monitoring of aerosol optical properties hence their radiative characteristics and forcing to monitor their contribution to climate change.

This paper intends to contribute to the understanding of short term changes in radiative forcing of urban, rural and maritime atmospheres of Kenya.

## 2. Materials and Methods

### 2.1 Determination of Aerosol Optical Properties

Aerosol optical depth ( $\tau_\lambda$ ) was derived based on the Beer-Lambert-Bouguer law (Holben *et al.*, 1998)

$$V_\lambda = V_{0\lambda} D^{-2} \exp(-\tau_\lambda M) \quad (1)$$

where for each wavelength channel corresponding to different aerosol particle sizes,  $V_\lambda$  is the digital voltage measured by the sun photometer at a wavelength  $\lambda$ ,  $V_{0\lambda}$  is the extraterrestrial voltage at wavelength  $\lambda$  as modified by the relative Earth-Sun distance ( $D$ ) while  $M$  is the optical air mass.  $\tau_\lambda$  is the total optical depth at a particular wavelength ( $\tau_\lambda = \tau_{a\lambda} + \tau_{R\lambda} + \tau_{o3\lambda}$ ).  $\tau_{a\lambda}$  is the aerosol optical depth,  $\tau_{R\lambda}$  is the Rayleigh (air) optical depth component and  $\tau_{o3\lambda}$  is the ozone optical depth at a specific wavelength  $\lambda$  (Holben *et al.*, 1998). Direct sun photometric measurements include  $V_\lambda$ ,  $V_{0\lambda}$ ,  $D$  and  $M$  from which  $\tau_\lambda$  is derived.

## 2.2 Radiative Characteristics

The integrated flux (total spectral irradiance, TSI) and the equilibrium global mean surface temperature change ( $\Delta T_s = 3^\circ$ ) was used to derive radiative forcing over the study sites according to equation 6 below. Spectral irradiance  $E_o(z, \lambda)$ , is the radiant energy flux per unit time in a given wavelength interval. The irradiance is obtained by integrating the radiance, which is the radiative solar power per unit solid angle in a particular direction, weighted with the cosine of the viewing zenith angle,  $\mu = \cos\theta$  over all viewing directions in the hemisphere ( $2\pi$  steradians). The integration of spectral irradiance corresponds to the solar integrated fluxes (TSI or global irradiance) over the entire spectrum arriving at the top of the terrestrial atmosphere. The change in solar activity of the atmosphere causes a variation in the TSI which is related to the spectral irradiance ( $E_o(z, \lambda)$ ) as shown in Equation 2.

$$TSI = \int_0^{\infty} E_o(z, \lambda) d\lambda dz \quad (2)$$

where  $z$  and  $\lambda$  represent the height and wavelength respectively while the limits of integration can take on any desired wavelength range.

## 2.3 Description of Study Sites

The three sites at which this study was undertaken are: Malindi ( $2^\circ\text{S}, 40^\circ\text{E}$ ) representing a maritime region (altitude 12m), Mbita ( $0^\circ\text{S}, 34^\circ\text{E}$ ) representing a rural site dominated by agricultural and biomass burning (altitude 1125m) and Nairobi (an industrial city site) ( $1^\circ\text{S}, 36^\circ\text{E}$ ) (altitude 1650m). Nairobi's sun photometer proximity to the industrial area allows for systematic monitoring of aerosols and pollution in this fast expanding metropolis. These sites are shown in Figure 1.

## 2.4 Radiative Transfer Modeling

### 2.4.1 Brief Description of the COART Model

Coupled Discrete Ordinate Radiative Transfer (CDISORT) was used as a solver of radiative transfer problem by COART model. CDISORT accounts for the change in refractive

index at the layers interface. COART considers the atmosphere and ocean as one system and treats the ocean strata just as additional atmospheric layers with different optical properties. Similar to the atmosphere, the ocean can also be subdivided into an arbitrary number of layers required to resolve the vertical variations of water properties. COART models the absorption and scattering process in the atmosphere and ocean explicitly. This includes the scattering and absorption by molecules, aerosols, clouds, liquid water molecules and dissolved particulate matter in the ocean. Clouds have been ignored in this work.

COART calculates radiances and irradiances at any level of the atmosphere and ocean in both narrow and broad bands. For the narrowband spectra scheme, users can specify both the band (wavelength) limits and computational resolution arbitrarily. In this scheme, COART employs the LOWTRAN 7 band model (spectral resolution of  $20\text{ cm}^{-1}$ ) and the molecular absorption database for the atmosphere. This corresponds to a wavelength resolution of approximately 0.5 nm at 500 nm and 8 nm at 2000 nm. For efficient broadband calculations of radiance and irradiance, COART divides the solar spectrum ( $0.2\text{--}4.0\ \mu\text{m}$ ) into 26 fixed wavelength intervals; in each spectral interval, the k-distribution technique parameterizes molecular absorption in the atmosphere using the HITRAN 2000 database (Kato *et al.*, 1999). In this work, it was assumed that the depth into the ocean is zero so as to let COART be used for the atmosphere-land system hence all parameters in equations 3 to 5 that seem to be relevant only in the case of an ocean are all ignored by COART so as to assume an atmosphere land system with the land being flat.

### 2.4.2 Radiative Transfer Equation

The basic equation describing the radiative field through a plane-parallel medium is given by Zhonghai *et al.*, (1994) and Zhonghai *et al.*, (2006).

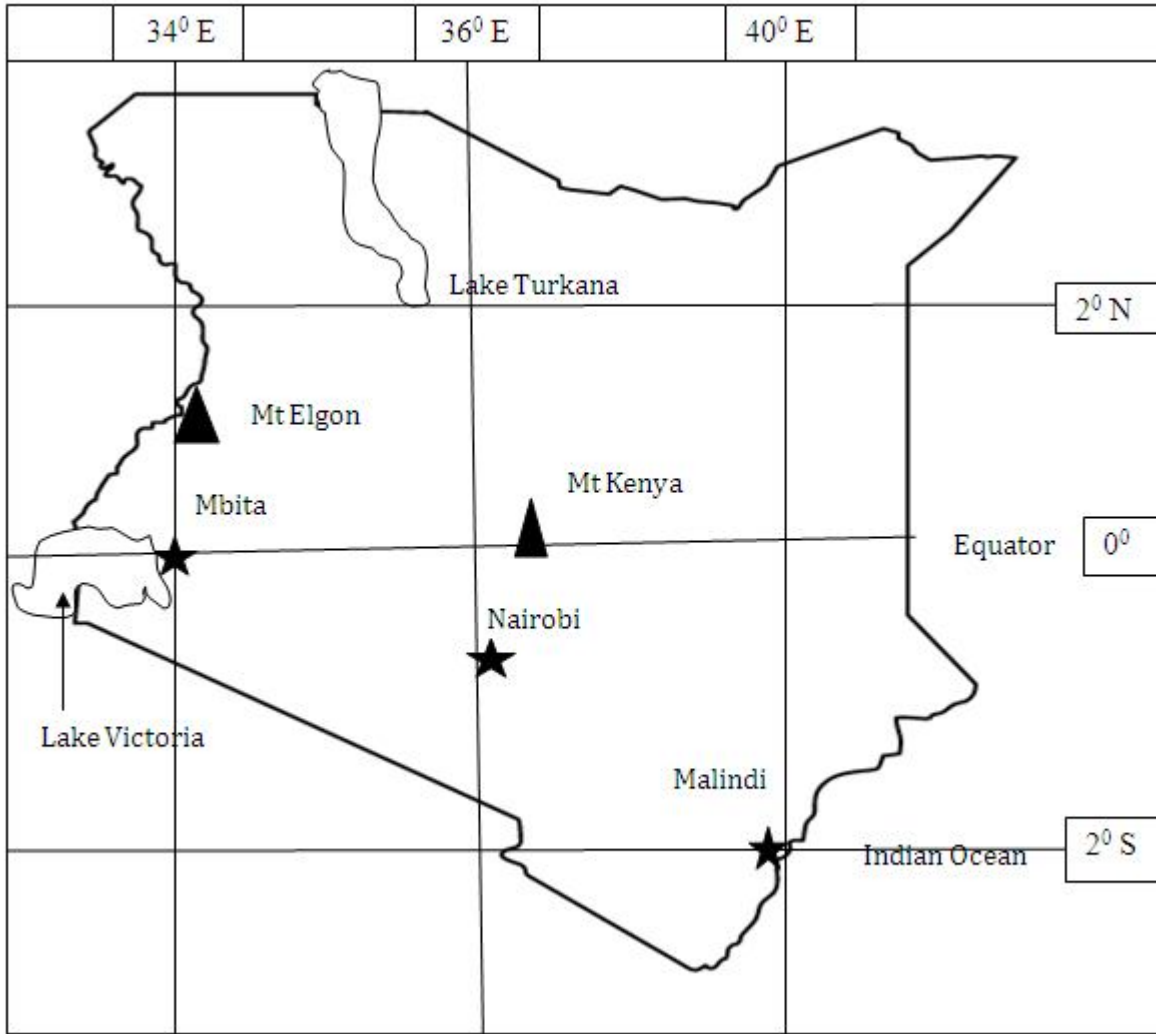


**Fig 1:** Map indicating the three AERONET sites of study in Kenya

$$\mu \frac{dI(\tau, \mu, \Phi)}{d\tau} = I(\tau, \mu, \Phi) - S(\tau, \mu, \Phi) \quad (3)$$

where  $I(\tau, \mu, \Phi)$  is the specific solar intensity (radiance) at a vertical optical depth  $\tau$  (measured downward from the upper boundary) in the direction  $(\mu, \Phi)$  ( $\mu$  is the cosine of the polar angle which is positive to the upward normal and  $\Phi$  is the azimuthal angle). The source function  $S(\tau, \mu, \Phi)$  is given by Equation 4

$$S(\tau, \mu, \Phi) = \frac{\omega(\tau)}{4\pi} \int_{-1}^1 P(\tau, \mu, \Phi, \mu', \Phi') I(\tau, \mu', \Phi') d\mu' + Q(\tau, \mu, \Phi) \quad (4)$$

$$Q_{air}(\tau, \mu, \Phi) = \frac{\omega(\tau)}{4\pi} F_0 P(\tau, \mu, \Phi) - \mu_0, \Phi_0 \exp\left(\frac{-\tau}{\mu_0}\right) + \frac{\omega}{4\pi} F_0 R(-\mu_0, \eta) P(\tau, \mu, \Phi, \mu_0, \Phi_0) \exp\left[-\frac{2\tau_a - \tau}{\mu_0}\right] \quad (5)$$

Where  $\mu_0$  is the cosine of the solar zenith angle and is positive,  $\Phi_0$  is the azimuthal angle for incident solar beam, and  $F_0$  is the solar beam intensity at the top of the atmosphere. The sym-

Where  $\omega(\tau)$  is the scattering albedo,  $P(\tau, \mu, \Phi, \mu', \Phi')$  is the phase function and  $Q(\tau, \mu, \Phi)$  represents the actual internal source. The symbols  $\mu$  and  $\Phi$  are the cosine of the polar angle and azimuthal angle of subsequent scattered or absorbed solar radiation respectively. The solar beam source in the atmosphere is expressed by Equation 5

bol  $\eta$  is the index of refraction of the land surface relative to the atmosphere and  $\tau_0$  is the total optical depth of the atmosphere. The first term in Equation 5 represents the contribution

from the upward beam source reflected at the atmosphere-ocean interface because of the Fresnel reflection caused by the change in the refractive index between air and sea water.  $R(\mu_o, \eta)$  is the ocean surface reflectance for the solar beam. For the purpose of simplification, several assumptions were made in this work to obtain a solution with a high degree of generality that can be used for solving real problems. Below are the assumptions under which COART model solves the radiative transfer equation:

- Only solar radiation is considered since it is strongly affected by the change in the refractive index due to aerosols and exhibits a much different transfer process in the coupled system. The emission is neglected for us to obtain a homogeneous solution.
- The specific intensity (radiance) is assumed to undergo anisotropic scattering and absorption of radiation in the coupled system.
- The land surface is assumed to be flat so as to neglect other radiative effects caused by the roughness of the surface by setting the wind speed to 0 m/s. A depth of 0 m assumes a land case with a vegetation cover of chlorophyll content of 0.2 mg/m<sup>3</sup>.
- The atmosphere-land system has uniform optical properties since the system is not vertically stratified (single layered).
- Atmospheric perturbations are as a result of aerosols only with other atmospheric species well taken care of by correcting their influences from those of the optical properties used.
- The Radiative Transfer Equation (RTE) is solved in a plane-parallel geometry.
- The reflectance values obtained in this case are a combination of both surface and aerosol contribution that is similar to the case when determined by other standard methods

By applying the above assumptions in solving Equation 3 together with appropriate quadrature and the discrete ordinate method as a solver, a general solution for the RTE that is suitable for the

single layer coupled system can be obtained (Zhonghai *et al.*, 1994). The general solution is the sum of both the homogeneous and particular solutions of Equation 3 with the boundary conditions applied according to the COART model.

## 2.5 Radiative Forcing Concept

Radiative Forcing (RF) is the change in net irradiance at the tropopause after allowing for stratospheric temperatures to re-adjust to a radiative equilibrium, but with the surface and tropospheric temperatures and state held at the unperturbed values (Ramaswamy *et al.*, 2001). A change in the net irradiance at the tropopause is of first order, a good indicator of the equilibrium global mean surface temperature change ( $\Delta T_s$ ).  $\Delta T_s$  is related to the RF by Equation 6 defined as:

$$\Delta T_s = \Omega \cdot RF \quad (6)$$

where  $\Omega$  is the climate sensitive parameter (integrated fluxes) over the study sites.  $\Delta T_s = -3^\circ\text{C}$  as estimated in the Fourth Assessment Report of the Intergovernmental Panel on Climate Change (IPCC). RF is expressed in terms of  $^\circ\text{C}/\text{Wm}^{-2}$  or  $\text{K}/(\text{Wm}^{-2})$

## 3. Results and Discussion

### 3.1 Integrated Fluxes

Integrated Fluxes (IF) correspond to the integrations of spectral irradiance arriving at the top of the terrestrial atmosphere over the entire spectrum. Integrated Fluxes was determined in the spectral range 440-1020 nm with a resolution of 10 nm using the COART model. The input parameters were aerosol optical depths ( $\tau$ ), single scattering albedo ( $\omega$ ) and asymmetry factor ( $g$ ) computed in the AEROSOL ROBOTIC NETWORK (AERONET) framework. The variation of downward and upward integrated fluxes with optical air masses for all the study sites was similar to that shown for Nairobi in 2008 (Figure 1a-b).

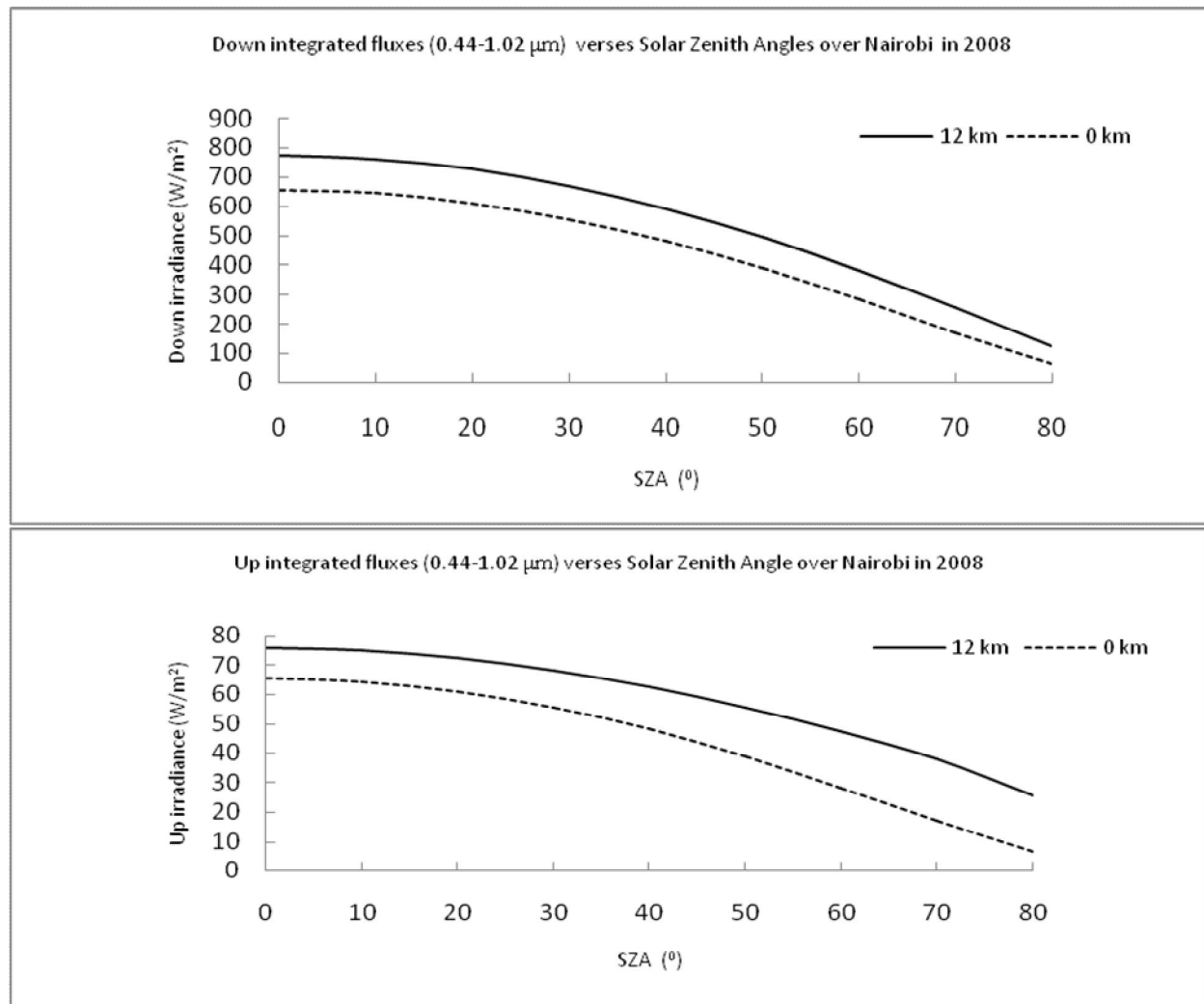


**Fig 1a-b:** Modeled integrated fluxes of down and up irradiance at 12 km and 0 km above sea level for varying Solar Zenith Angles respectively over Nairobi in 2008

The 12 km atmospheric altitude was considered since it is the standard height at which air craft emissions into the atmosphere are prevalent. Also, the tropopause has its average altitude value at this point; here, aerosol concentration is known to be highest as assumed by many radiative transfer models (IPCC, 2001).

From Figure 1, we note that both downwards and upwards integrated irradiance decrease with increasing optical air mass factor increasing optical air mass factor (increasing SZAs). The net downward and upward integrated irradiance (their respective differences between the two atmospheric levels) over Nairobi (2006-2008) was noted to vary inversely with aerosol number densities as noted in both Tables 1 and 2. Variations in

net downward and upward integrated fluxes at zero SZA together with the up/downward ratio are shown in Table 1 for the periods of study. Variations in integrated fluxes over Nairobi at the two atmospheric levels reflect the variation in aerosol number densities as indicated in Tables 1 and 2. An increase in aerosol number densities in the wavelength channels under consideration from 2006-2007 time interval translates to an increase in the up/down integrated flux ratio of about 3.1%. Thus, an increase in aerosol number concentration increases attenuation of incoming solar radiation through absorption and scattering of the incoming solar radiation. On the other hand, a decrease in aerosol number density from 2007-2008 translates to a decrease in the ratio of 6.8% since incoming

**Table 1:** Variation in net integrated fluxes at the two atmospheric levels over the study sites.

Site	Year	Net downward integrated irradiance ( $W/m^2$ )	Net upward integrated irradiance ( $W/m^2$ )	Up/down
Nairobi	2006	121.98	12.89	0.1065
	2007	103.24	11.33	0.1098
	2008	118.38	12.09	0.1023
Mbita	2007	114.36	11.97	0.1047
Malindi	2008	130.76	14.15	0.1082

solar radiation attenuation is enhanced between the two atmospheric levels. We note that the up to down ratio in Table 1 remains virtually constant over the study sites. This implies that the radiant flux lost due to the presence of aerosols in the entire spectrum under consideration over the three study sites is almost the same and significant changes can only be noted after a full solar cycle. Likewise, an increase in aerosol number densities from 2006 to 2007 over Nairobi translates to an increase in the radiant flux lost due to incoming solar radiation attenuation from the atmosphere as noted in the up/down ratio from Table 1. The ratio remains relatively constant

over the three sites of study; hence flux energy lost over the atmospheres from the sites of study is almost constant.

Note that an appreciable variation in the aerosol number densities over Nairobi was dominated by aerosol particles in the 675 nm and 870 nm wavelength channels. A significant aerosol number density increase of 45.7 % and 49.5 % in both 675 nm and 870 nm wavelength channels respectively is noted for 2006-2007. This is attributed to a decrease in amount of rainfall events (of about 13.8%) which limits aerosol removal processes through washout in 2006-2007. A decrease of 7.7% and 54 % in the same wavelength channels is also revealed

**Table 2:** Average Aerosol Number Density Distribution over the Study Sites

Site	Year	Average aerosol Number Density (N) $\times 10^7/cm^3$						
		340 nm	380 nm	440 nm	500 nm	675 nm	870 nm	1020nm
Nairobi	2006	16.24	11.89	8.35	6.88	1.97	1.02	1.10
	2007	24.58	16.52	11.55	8.16	3.63	2.02	1.35
	2008	19.81	15.04	9.87	7.14	3.35	1.85	1.35
Mbita	2007	24.22	16.86	11.23	8.67	3.97	1.52	0.98
Malindi	2008			13.8		4.47	2.53	1.71

for 2007-2008 period; this is attributed to an increase of about 14.1% of rainfall received over Nairobi in the same period. Aerosol number densities are thus important modulators of radiative forcing since they influence the variation in the integrated fluxes and hence the climatic system under study.

### 3.2 Radiative Forcing Impacts due to Atmospheric Aerosols

A positive change in the flux implies a warming effect on the Earth by the sun and vice versa for effect on the Earth by the sun and vice versa for a negative flux. Radiative forcing effects of aerosol particles on the surface of the Earth for the studied sites was accomplished by use of Equation 6 at zero SZA; the results are shown in Table 3.



Radiative forcing impacts due to aerosols remain virtually constant throughout the study period over Nairobi (2006-2007). Like wise, Mbita and Malindi reflect almost the same values as Nairobi. This implies that the impact of changes in secular climate drivers in these case aerosols on radiative forcing is almost uniform over the three sites and is approximated as  $K/(W/m^2)$ . Consequently, it may be assumed to be

uniform over Kenya. This value is lower as compared to the combined global anthropogenic radiative forcing estimated to be  $+1.6 [-1.0, +0.8] W/m^2$  by Forster *et al.* (2007). It is also important to note that radiative forcing due to aerosol is always negative since most of the dominating attenuation processes of the incoming solar intensity is scattering.

**Table 3:** Radiative Forcing due to Aerosol Particles over the Study Sites

Site	Year	Net Integrated Flux ( $W/m^2$ )	Radiative Forcing $K/(W/m^2)$
Nairobi	2006	592.74	-0.46
	2007	601.29	-0.45
	2008	590.46	-0.46
Mbita	2007	593.73	-0.46
Malindi	2008	578.97	-0.47

#### 4. Conclusions

The radiant flux lost in the entire spectrum under consideration remained constant resulting to a radiative forcing effect that is relatively constant for all three sites under consideration despite the observed differences in the various aerosol particle properties i.e. physical, mode of generation, chemical and number densities dominating the sites. Up/down integrated flux ratio remained virtually constant for 2006-2008 over the study sites. Utilizing the integrated fluxes, radiative forcing due to atmospheric aerosols was estimated, and found to remain relatively constant at  $-0.46 K/(W/m^2)$  a value slightly lower as compared to the combined global anthropogenic radiative forcing estimated to be  $+1.6 (-1.0, +0.8) W/m^2$  for all the three sites despite the observed differences in the various aerosol particle properties dominating the sites. The radiative forcing estimate due to atmospheric aerosols will be key in the development of climate models that are used for prediction of climate change and modeling of aerosol impact on environmental pollution over the study sites in Kenya. The radiative forcing estimate due to atmospheric aerosols

will be key in the development of climate models that are used for prediction of climate change and modeling of aerosol impact on environmental pollution over the study sites in Kenya.

#### Acknowledgements

The optical data derived from AERONET Network sun photometers were kindly supplied by Brent Holben and staff of Federated Instrument Network and Data Archive. We wish to offer our sincere gratitude to all NASA officials particularly Dr. Thomas Charlock and Dr. Zhonghai Jin (online COART model) and Steve Kempler (MODIS satellite data) and their staff for maintaining and allowing us to use the NASA Goddard Earth Sciences (GES) data and information needs for that made this work a success. Meteorological data was obtained from the Kenya Meteorological Department. The University of Nairobi provided the Master of Science scholarship without which this work could not have been achieved.

## References

- Alpert, P., Kaufman, Y.J., Shay-el, Y., Tanre, D., Da Silva, A. and Joseph, Y.H. (1998). Dust forcing of climate inferred from correlation between dust data and model errors, *Nature*. **395**, 367-370.
- Badarinath, K. V. S., Sharma, A. R. and Shailesh, K. M. (2009). Impact of emissions from anthropogenic sources on satellite-derived reflectance, *Advances in Space Research*, **43**, 1545-1554.
- Bowman, K and Krueger, A (1985). A global climatology of Total Ozone from the Nimbus 7 Total Ozone Mapping Spectrometer, *J Geophys. Res.* **90**, 7967-976.
- Forster, P., Ramaswamy, V., Artaxo, P., Bernsten, T., Betts, R., Fahey, D.W., Haywood, J., Lean, J., Lowe, D.C., Myhre, G., Nganga, J., Prinn, R., Raga, G., Schulz, M. and Van Dorland, R. (2007): Changes in Atmospheric Constituents and in Radiative Forcing. In: Climate Change 2007: The Physical Science Basis. Contribution of Working Group 1 to the Fourth Assessment Report of the Intergovernmental Panel on Climate Change [Solomon, S., Qin, D., Manning, M., Chen, Z., Marquis, M., Averyt, K.B., Tignor, M. and Miller, H. L. (eds)]. Cambridge University Press, Cambridge, United Kingdom and New York, NY, USA.
- Ghan, S. J., McFarquhar, G., Korolev, A., Liu, P., Strapp, W., Verlinde, H. and Wolde, M. (2008). ISDAC Flight Planning Document, DOE/SC-ARM-0801.
- Hansen, J., Sato, M. and Ruedy, R. (1997). Radiative forcing and climate response, *J Geophys. Res.* **102**(D6), 6831-6864.
- Hatzianastassiou, N., Katsoulis, B. and Vardavas, L. (2004) Sensitivity analysis of aerosol direct radiative forcing in ultraviolet-visible wavelengths and consequences for the heat budget, *Tellus* **56B** 368-381.
- Haywood, J.M., Roberts, D.L., Slingo, A., Edwards, J.M. and Shine K.P. (1997). General circulation model calculation of the direct radiative forcing by anthropogenic sulfate and fossil fuel soot aerosols. *J. climate*, **10**, 1562-1577.
- Holben, B. N., Eck, T.F., Slutsker, I., Tanre, D., Buis, J.P., Setzer, A., Vermote, E., Reagan, J.A., Kaufman, Y.J., Nakajima, T., Lavenu, F., Jankowiak, I. and Smirnov, A. (1998). AERONET-A federated instrument network and data archive for aerosol characterization, *Remote sens. Environ.* **66**, 1-16.
- Holben, B. N., Eck, T.F., Slutsker, I., Tanre, D., Buis, J.P., Setzer, A., Vermote, E., Reagan, J.A., Kaufman, Y.J., Nakajima, T., Lavenu, F., Jankowiak, I. and Smirnov, A. (2001). An emerging ground based aerosol climatology: Aerosol optical depth of AERONET, *J. Geophys. Res.* **106**, 12067-12097.
- Intergovernmental Panel on Climate Change (IPCC). (2001). Climate Change 2001: *The specific basis. Contribution of working group 1 for the third assessment report*. Houghton, J.T., Ding, Y., Griggs, D. J., Noguer, M., Van der Linden, P. J., Dai, X., Maskell, K., Johnson, C. A. (eds.) Cambridge University Press: UK.
- Johnson, B.T., Christopher, S., Haywood, J.M., Osborne, S.R., McFarlane, S., Hsu, C., Salustro, C. and Kahn, R. (2009). Measurements of aerosol properties from aircraft, satellite and ground-based remote sensing: A case study from the Dust and Biomass-burning Experiment (DABEX). *Q.J.R. Meteorol. Soc.* D01: 10.1002/qj.420.
- Kato, S., Ackerman, T.P., Mather, J.H., and Clothiaux, E.E., (1999) The K-distribution method and correlated-k approximation for shortwave radiative transfer model, *J. Quant. Spectrosc. Radiat. Transfer* **62**, 109-121.
- Myhre, G., Stordal, F., Restad, R. and Isaksen I. S. A. (1998). Estimates of the direct radiative forcing due to sulfate and soot aerosols *Tellus*, 50B, 463-477.
- Ramaswamy, V., Boucher, O., Haigh, J., Hauglustaine, D., Haywood, J., Myhre, G., Nakajima, T., Shi, G. Y. and Solomon, S. (2001): Radiative forcing of climate change. In: Climate change in 2001: The Specific Basis. Contribution of the working group 1 to the Third Assessment Report of the IPCC [Houghton et. al. (eds.)]. Cambridge University Press, United Kingdom and New York, NY, USA, 349-416.

- Twomey, S. (1991). Aerosol, cloud and Radiation, *Atmos. Environ.*, **25**, 2435-2442.
- Wickland, E.D. (1991). Mission to planet Earth: The ecological perspective, *ecology*. **72**(6), 1923-1933.
- Wittrock, F., Oetjen, H., Richter, A., Fietkau, S., Medeke, T., Rozanov, A. and Burows, J.P. (2004) MAX-DOAS measurements of atmospheric trace gases in Ny-Ålesund-Radiative transfer studies and their application, *Atmos. Chem. Phys.*, **4**, 955-966.
- Woods, T.N. and Rottman, G.J. (2002) Solar ultraviolet variability over time periods of aeronomical interest. In: Mendillo, M., et al (Eds) *Comparative Aeronomy in the Solar System*. American Geophysical Union Monograph.
- Zhonghai, J. and Stamnes, K. (1994). Radiative transfer in nonuniformly refracting layered media: Atmosphere-ocean system, *Applied optics*, **33**, No. 3: 431-442.
- Zhonghai, J., Thomas, P., Charlock, Rutledge, K., Stamnes, K. and Yingjian, W. (2006). Analytical solution of radiative transfer in the coupled atmosphere-ocean system with a rough surface. *Optics*, **45**, No. 28: 7443-7455.